

Role of ambient gas on laser-ablated plumes for thin carbon film deposition

R. K. Thareja,* R. K. Dwivedi, and Abhilasha

Department of Physics and Centre for Laser Technology, Indian Institute of Technology, Kanpur 208 016, India

(Received 5 April 1996; revised manuscript received 19 August 1996)

We report the role of ambient gas on the laser-ablated carbon plume used for carbon-film deposition. An attempt is made to correlate the characteristics of deposited film with the optical emission of various species in the laser-ablated carbon plume. We have deposited thin carbon films on silicon substrate using 0.532 and 0.355- μm laser wavelengths at low fluence in the presence of helium and argon gases. The deposited films were characterized by scanning electron microscopy, transmission electron microscopy, selected area electron diffraction, x-ray diffraction, and Raman spectroscopy. The structure and the surface morphology of the deposited films were found to be strongly dependent on the choice and pressure of the ambient gas. The presence of carbon clusters (fullerenes) in laser-ablated carbon "soot" in a helium atmosphere was confirmed by UV-visible and infrared spectroscopy. [S0163-1829(97)03004-X]

I. INTRODUCTION

Laser-ablation deposition (LAD), also known as pulsed-laser deposition (PLD) has found an increasing interest in recent years in depositing a variety of materials including metals, semiconductors, insulators, and superconductors.¹ The flux of the material to be deposited in PLD is generated by irradiating an appropriate target with a high-intensity beam of pulsed-laser light, and a film is grown by collecting this flux onto a suitably placed substrate. The deposited flux can be modified by changing the ambient conditions, e.g., background gas and/or plasma. Despite its growing importance, the microscopic details of the processes responsible for some of the characteristic features of PLD are not well understood. The evaporation of the deposited material, plasma formation, and the interaction of vapor/plasma species with the background gas are believed to be relevant in determining the film structure and morphology. The presence of an ambient gas can affect both the nature and energy of the species impinging on the film growth surface, which in turn controls the characteristics of the deposited films. The characteristics of the laser-deposited films depend on, among the other experimental parameters, the laser fluence, wavelength, and background gas pressure.²⁻⁵

It is well known that the laser-ablation produces several species in the plume such as neutral atoms, molecular clusters, or highly excited atoms and ions, depending on the laser fluence.⁶ The presence of ambient gas greatly influences the plasma plume.⁷ Therefore, the study of the ablated plumes with background gas is interesting not only to obtain a better understanding of the mechanism involved, but also to control and optimize the PLD process.

In the PLD process, the laser wavelength used for ablation also plays a dominant role in defining the characteristics and morphology of the deposited films. Surface morphology is the most important factor determining the possibility of thin films for device applications. The choice of a right wavelength and fluence helps to minimize the formation of particulate on the film surface. It has been claimed that the pulsed-laser deposition of high- T_c superconductors using shorter wavelengths yields superior quality films.⁸ The car-

bon films grown using various wavelength laser radiations exhibit increasing diamond character with decreasing wavelength.⁵

The intense laser-beam-created plasmas have electrons and ions in addition to copious amount of neutrals. However, at moderate and low intensities the clusters are also formed in addition to electrons, ions, and neutrals. The neutral species play a vital role in the film growth in general. The number density of these species depend on irradiation conditions, collision kinetics in the plume, and the distance from the target surface. Earlier, we reported the formation of fullerenes C_{60} , C_{70} , and C_{84} in the laser-ablated carbon.⁹ The study of carbon clusters (fullerenes) has attracted attention since Kroto *et al.*¹⁰ discovered them in 1985, and Kratschmer *et al.*¹¹ succeeded in synthesizing them in 1990. The discovery of conductivity in alkali-metal-doped C_{60} (and C_{70}) and superconductivity in C_{60} doped with K ($T_c = 18$ K), Rb ($T_c = 28$ K), and their alloys has added further excitement in C_{60} thin films.¹² The fabrication of C_{60} thin films attracts attention not only because of their basic properties but also for their possible application to electronic devices such as solar cells.¹³ However, the dynamics of formation of carbon clusters, in particular C_{60} and C_{70} , is still not well understood. Weiske *et al.*¹⁴ reported the fragmentation of C_{60}^+ and C_{70}^+ to C_n ($n=2, 4, 6, \text{ and } 8$) on collision with H_2 , D_2 , and Ar. Recently Gruen *et al.*¹⁵ reported obtaining C_2^* and C_2 species by fragmentation of C_{60} in a microwave discharge in a 1-Torr argon atmosphere. We reported the optical emission diagnostics of carbon plasma plumes used for film deposition at various laser wavelengths, laser irradiances, and ambient gas pressures.^{2,3,16-18} The emission spectra showed atomic/ionic species at high laser irradiances of all laser wavelengths. However, the molecular C_2 emission dominated the spectrum at low irradiances ($\sim 10^8 - 10^9$ W/cm²), where the formation of diamondlike carbon has been reported.^{19,20} At this irradiance, deposition of high- T_c superconductors,⁸ cluster production,²¹ etc. has also been reported. It has been shown that the doping of N_2 during the deposition of carbon films degrades the diamondlike properties but improves the interface adhesion and intrinsic stress in the film.¹⁹

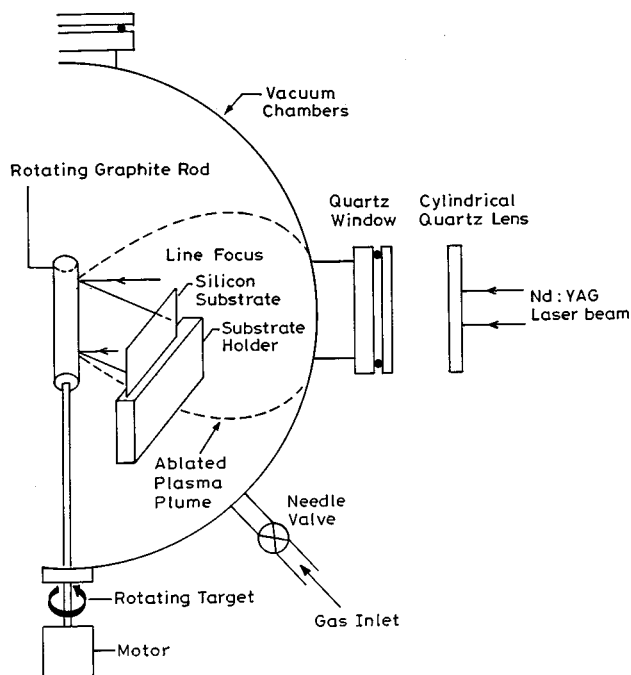


FIG. 1. Experimental setup used for deposition of carbon films.

In general, the properties of the carbon films prepared by the laser-ablation deposition technique range from soft and graphitic to hard and diamondlike, depending on laser power and wavelength as well as background gas conditions. Here we present results for the characterization of pulsed-laser-deposited thin carbon films from carbon plumes using 0.532- and 0.355- μm laser fluences in helium and argon atmospheres. To the author's knowledge, this is the first report on the correlation of characteristics of the deposited film with properties of the laser-ablated plume.

II. EXPERIMENTAL DETAILS

The experimental setup used for the deposition of the carbon films is shown in Fig. 1. A Nd:YAG (yttrium aluminum garnet) (DCR-4G) laser and its harmonics, delivering up to 1 J in 8 ns at its fundamental at 10 pps, were used for the present study. The laser beam was line focused onto the graphite target enclosed in a vacuum chamber, using a cylindrical lens of focal length 25 cm. A graphite target rod was continuously rotated and translated so that the laser always encounters a fresh surface. The chamber was evacuated to a pressure better than 10^{-3} Torr, and then backfilled with the required gas. The experiment was carried out for different pressures in the range 10^{-2} –100 Torr of helium and argon gas. The ablated carbon was deposited on silicon and glass substrates placed 1 cm from and parallel to the target surface. The deposition time (20 min) was kept constant for depositing films at various wavelengths and ambient pressures. The deposited films at different ambient gas pressures were characterized by scanning electron microscopy (SEM), transmission electron microscopy (TEM), selected area electron diffraction (SAED), x-ray diffraction (XRD), and micro-Raman spectroscopy. "Soot," the ablated carbon powder, collected from the chamber at different gas pressures, was dissolved in benzene/*n*-hexane solution, and the soluble material charac-

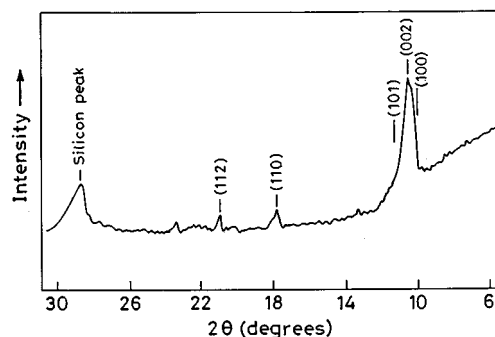


FIG. 2. X-ray-diffraction pattern of the carbon film deposited at 100-Torr helium gas pressure using a 4.68-J/cm² fluence of a 0.532- μm laser wavelength. Peaks at 10.3°, 11°, 17.9°, and 21° show the presence of (100), (002), (110), and (112) crystalline planes of C₆₀.

terized by UV-visible and IR spectroscopy.⁹ Under similar conditions of deposition of the carbon films, the plasma radiation was imaged onto the monochromator, and was detected with a photomultiplier tube and recorded on a strip chart recorder or displayed on the oscilloscope to observe C₂ emission.^{2,3}

III. RESULTS AND DISCUSSION

The structural properties of the deposited carbon films were investigated by x-ray diffraction using a standard $\theta/2\theta$ diffractometer (Cu $K\alpha$ radiation) in order to determine crystalline orientation. Figure 2 shows the typical XRD pattern of the carbon film deposited on silicon substrates at 100-Torr helium pressure using 4.68-J/cm² fluence of 0.532- μm laser radiation. Peaks at 10.3°, 11°, 17.9°, and 21° show the presence of (100), (002), (110), and (112) crystalline planes of C₆₀. X-ray diffraction was done for the carbon films at various helium pressures ranging from 10^{-2} to 100 Torr, and it was found that these peaks were prominent only at 100 Torr. At lower helium pressures (less than 100 Torr) the films were amorphous. An increase in helium pressure up to 100 Torr improved the quality of the film crystallization and phase orientation.

Figure 3 shows the SEM images of the carbon films deposited on silicon substrates at various helium gas pressures using a 4.68-J/cm² fluence of 0.532- μm laser radiation. The figure shows the effect of helium gas pressures on the morphology of the films. The surface morphology of the films changed dramatically with increasing helium gas pressures, with densely packed spherical features dominating the film. The nucleation density of the carbon clusters increased with an increase in helium gas pressure up to 100 Torr. However, beyond 100 Torr, the carbon film started peeling off, and showed a "cauliflower" morphology with no systematic pattern. This variation in the morphology of the films is attributed to the temperature variations of various species in the laser-ablated carbon plume at various helium pressures. The comparison of individual microcrystals obtained at 100-Torr helium pressure and in vacuum, respectively, showed that in vacuum the assemblage of hexagonal crystals was dominant,

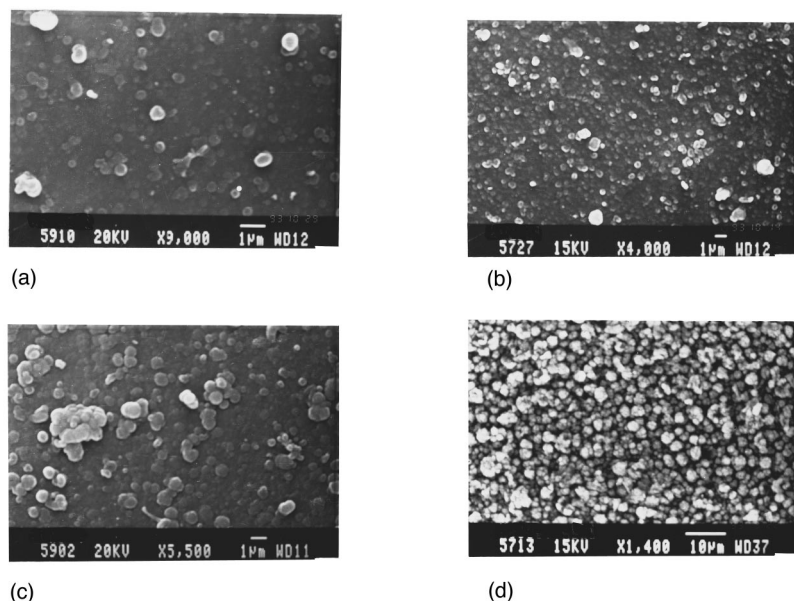


FIG. 3. SEM images of laser-ablated carbon films at helium gas pressures of (a) 10^{-2} , (b) 1, (c) 10, and (d) 100 Torr.

whereas in the presence of helium gas, particularly at 100 Torr, spherical aggregates of carbon were dominant.²²

To confirm the formation of C_{60} clusters, the carbon soot was collected from the deposition chamber at various helium gas pressures at 4.68 J/cm² fluence of 0.532- μ m laser radiation. Figure 4 shows the optical-absorption spectrum recorded at room temperature from *n*-hexane solvable carbon soot in the range 200–450 nm. The spectra showed peaks around 211, 231, 273, and 299 nm, and a broad band at 325 nm. These peaks are characteristic of C_{60} and C_{70} clusters.²³ The peak at 231 nm appears as a shoulder to 211 nm. The benzene dissolvable fullerenes were further characterized using vibrational spectroscopy. Since the Raman spectral studies showed very few crystalline domains, we resorted to the method of extracting fullerenes by dissolving the ‘soot’ in benzene and depositing the aliquots of the benzene extract onto KBr pellets for IR spectroscopy. We did not make any attempt to separate out the clusters as the yield of the benzene soluble clusters was very low, thus an overlapping of many bands in the IR spectra is expected. Figure 5 shows the IR spectra recorded for the soot collected at different helium gas pressures using 0.532- μ m laser irradiation. The spectra showed that the modes became more prominent as the helium gas pressure was increased from 10^{-2} to 100 Torr. The modes were observed at 1462, 1126, 739, 701, 670, 651, 575, and 525 cm⁻¹, which could be due to C_{60} and C_{70} . The observed bands were identified by comparison with ear-

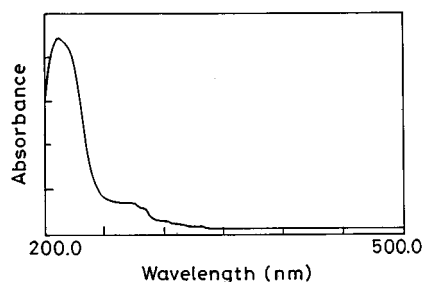


FIG. 4. Optical-absorption spectrum in the range 200–450 nm.

lier work.¹¹ In addition, a strong mode at 1720 cm⁻¹ was observed in the IR spectrum, showing the presence of higher fullerenes greater than C_{70} .

There are several reports explaining the growth mechanism of fullerenes.²⁴ Wakabayashi and Achiba²⁵ proposed a simple model to explain the formation mechanism of the stable fullerenes. Accordingly, for the I_h symmetry and closed caging of C_{60} molecule, C_2 is the dominant fragment. Our result of increasing nucleation density up to 100 Torr could well be correlated with increase in yield of C_2 species in our experiment. It is found that at higher laser fluence the plasma emission is dominated by atomic/ionic species from

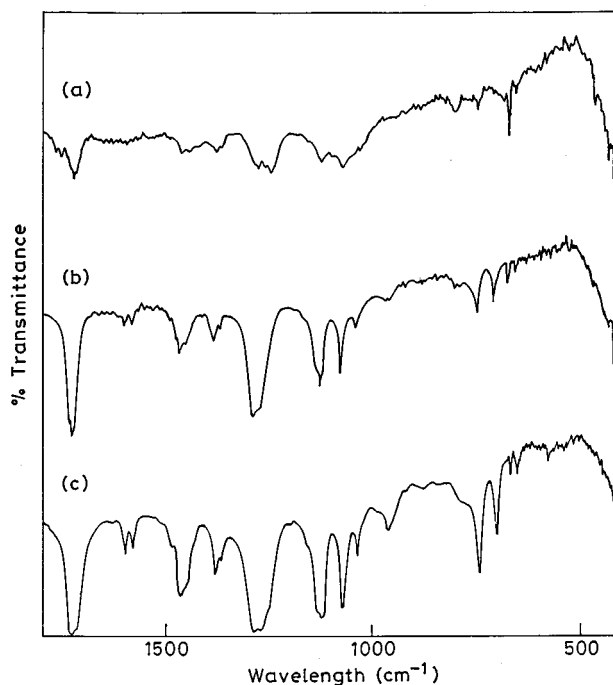


FIG. 5. Infrared spectra of carbon clusters extracted from benzene solvable soot collected at (a) 10^{-2} , (b) 1, and (c) 100-torr helium pressure.

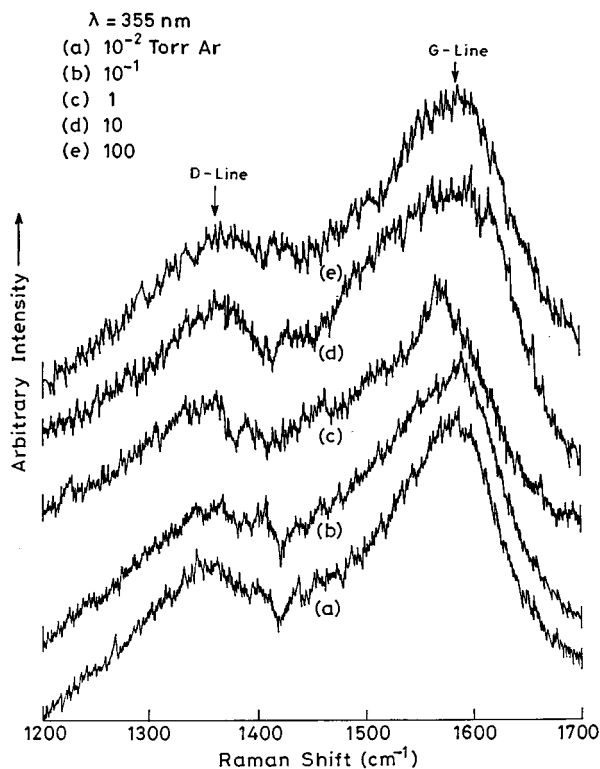


FIG. 6. Micro-Raman spectra for carbon films at various argon gas pressures using a 1.90-J/cm^2 laser fluence of a $0.355\text{-}\mu\text{m}$ laser wavelength.

C V to C I and at low fluence molecular C_2 emission is dominant. Moreover, in the presence of ambient gas a significant enhancement for ionic, atomic, and molecular species of carbon was observed. Characterization of the deposited films along with the soot showed that the yield of fullerenes formation initially increased with pressure, and then decreased after attaining a maximum as the pressure is increased beyond 100 Torr. The vibrational temperature calculated for C_2 species using band head intensities of C_2 Swan bands in the presence of helium gas decreased with increasing helium gas pressure. This indicates that the presence of helium gas helps in the cooling and clustering of species, and in turn increases the dominance of higher carbon clusters (fullerenes) with increasing helium gas pressures.

The films deposited in the presence of various argon gas pressures at 1.90-J/cm^2 laser fluence of $0.355\text{ }\mu\text{m}$ showed altogether different behavior than those obtained in presence of helium. The surface morphology of the deposited films in the presence of argon gas showed the presence of various spherical-shaped protrusions of different diameters on the substrate surface. The nucleation density of the clusters on the substrate surface was found to be at a maximum at 1 Torr of argon gas pressure, while it decreased on either side with a change of argon gas pressures. The thickness of the film using SEM was found to be approximately $30\text{ }\mu\text{m}$ at 1-Torr argon gas pressure.

Figure 6 shows the micro-Raman spectra of the deposited films at various argon gas pressures. We observed the presence of two well-defined characteristic peaks in the spectrum at 1350 (D line) and 1580 cm^{-1} (G line). These peaks were attributed to disordered and graphitic carbon, respectively.²⁶

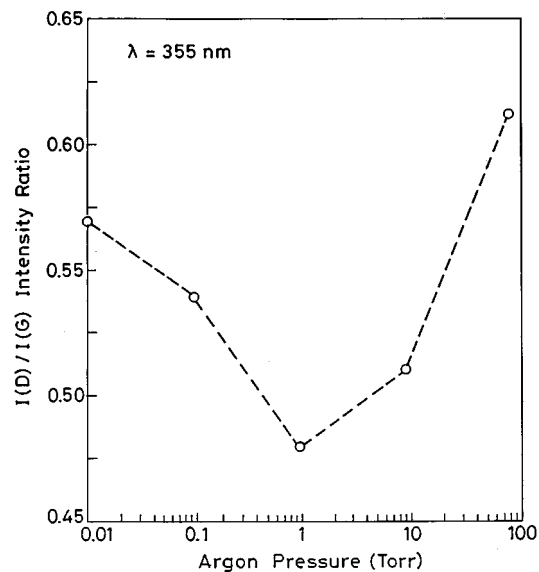


FIG. 7. Intensity ratio $I(D)/I(G)$ vs argon gas pressure for carbon films. The dotted line is only a guide to the eye.

However, the Raman spectra characteristic of diamond (sharp peak at 1332 cm^{-1}) were not obtained. It has been shown by several investigators that the large width of a 1350-cm^{-1} band can obscure the 1332-cm^{-1} band.^{27,28} As the sensitivity factors of diamond and nondiamond carbon relate as $\approx 1/60$,²⁶ therefore the nanocrystalline diamond nuclei present in the deposited film may be obscured by the broad nondiamond 1350-cm^{-1} peak due to this large sensitivity difference.

Two important features observed are (1) the decrease of the D -line-to- G -line intensity ratio $I(D)/I(G)$ as the argon pressure was increased up to 1 Torr, but its increase with further increase in argon gas pressure; and (2) the downward shift of the G line for the films deposited at 1-Torr argon gas pressure. Figure 7 shows the $I(D)/I(G)$ intensity ratio as a function of argon gas pressure. The ratio is found to be minimum at 1 Torr of argon gas pressure. It has been shown that the ratio $I(D)/I(G)$ varies inversely with the size of the graphite crystallites.²⁹ $I(D)/I(G)$ being at a minimum at 1 Torr indicates the presence of larger crystallites formed at 1 Torr compared to that formed at other pressures, agreeing well with SEM results.² The broad G line shifted to 1550 cm^{-1} for the film deposited at 1 Torr, a characteristic feature of diamondlike carbon. The width of the Raman lines were also seen to be lowest for the film deposited at 1 Torr of argon gas pressure. Thus the deposited film has the dominance of diamondlike carbon (DLC) character at 1 Torr of argon gas.

Figure 8 shows the XRD pattern of the film deposited at 1 Torr of argon gas pressure using a 1.90-J/cm^2 laser fluence of $0.355\text{-}\mu\text{m}$ laser wavelength. The peaks at 43.5° , 76° , 91.5° , and 120° indicate the presence of (111), (220), (311), and (400) crystalline planes of cubic diamond. It further confirms the formation of diamondlike carbon at 1-Torr argon pressure.

The TEM micrograph and the corresponding SAED pattern of the film deposited at 1-Torr argon using a 1.90-J/cm^2 laser fluence of a $0.355\text{-}\mu\text{m}$ laser wavelength is shown in Fig. 9. The diffuse intensity of the rings suggests the qua-

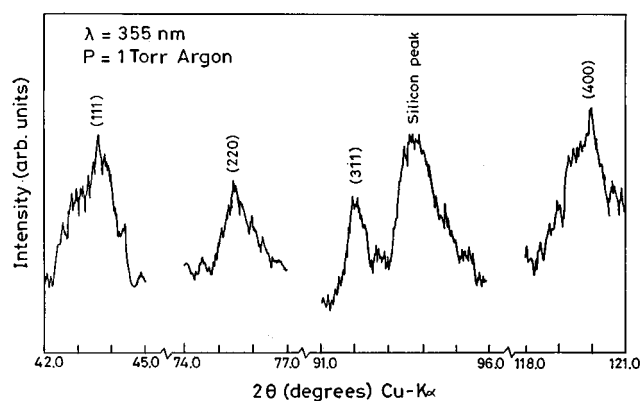
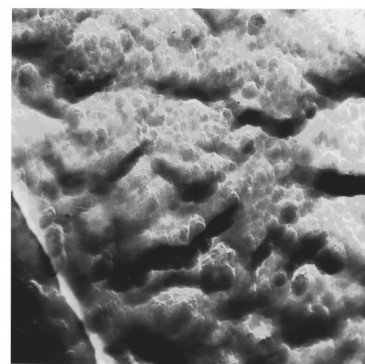


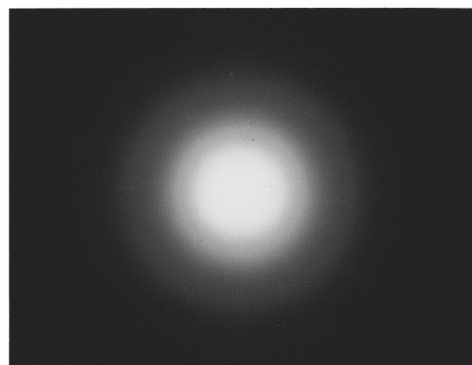
FIG. 8. X-ray-diffraction pattern of the carbon film deposited at 1-Torr argon gas pressure using a 1.90-J/cm^2 laser fluence of a $0.355\text{-}\mu\text{m}$ laser wavelength. Peaks at 43.5° , 76° , 91.5° , and 120° show the presence of (111), (220), (311), and (400) crystalline planes of cubic diamond.

microcrystalline nature of the film. The ring patterns represent typically polycrystalline face-centered-cubic material. Although diffraction rings are not clearly visible in Fig. 9(b) due to contrast limitations in the image, three rings are clearly visible in the negative. The d spacing of the rings were determined using the original negative, and compared well with the (111) and (220) planes of cubic diamond.³⁰ Therefore, we conclude that diamond is present in the film deposited at 1 Torr of argon.

To explain the above results, an extensive study of the optical emission from laser-ablated carbon plumes was undertaken. At a higher laser fluence, the plasma emission was dominated by atomic/ionic species from C V to C I, which recombine through atomic carbon away from the target. Temporally and spatially resolved studies of the emitted species were also performed. The electron temperature was estimated from the relative intensities of the spectral lines of different species. The electron temperature for C II species at 8 mm from the target is estimated to be ~ 2 eV in vacuum.⁶ The presence of a background gas had a strong influence on the plasma expansion process.⁷ In general, the interaction between laser plasma and the ambient gas influences parameters such as velocities of different species in the plume, density, and temperature of the species, which in turn control the characteristics of the deposited film. However, at the low fluence level used for thin film deposition, the optical emission from the plasma plume consists predominantly of molecular carbon. Spatially resolved studies of the plume at various ambient gas pressures ranging from 10^{-2} to 100 Torr showed that the intensity of molecular carbon band heads is at a maximum at around 3 mm from the target surface, and decreases very quickly beyond this distance. Molecular C_2 , which is the critical species for DLC, varies with the choice of and pressure of the ambient gas, in addition to the other laser parameters. We found that the intensity of C_2 Swan bands was greater in the presence of argon gas than of helium. It is known that the characteristics of the deposited films are effected by the energy of the species being deposited, which in turn is defined by the temperature of the species. Thus the temperature of the dominating species is a crucial parameter defining the characteristics of the film. In



(a)



(b)

FIG. 9. (a) TEM micrograph and (b) SAED pattern of the film deposited at 1-Torr argon using a 1.90-J/cm^2 laser fluence of a $0.355\text{-}\mu\text{m}$ laser wavelength.

order to optimize the film characteristics, the temperature of the dominant C_2 species in the plume was optimized. The vibrational temperature for C_2 species in the presence of helium gas show that the vibrational temperature decreases with increasing helium gas pressure. This indicates that the

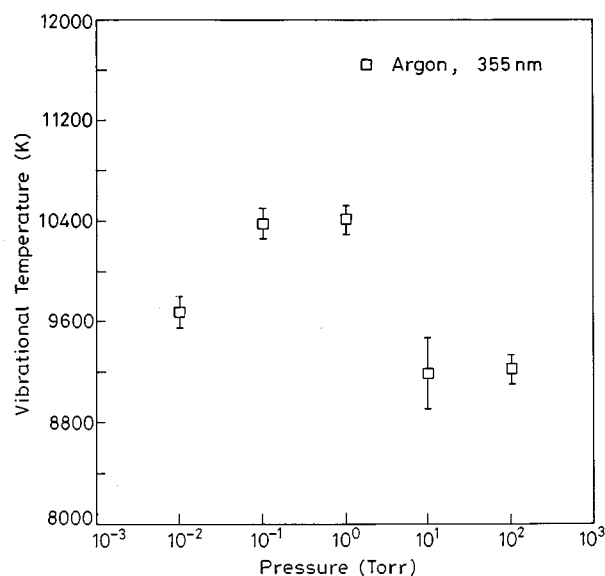


FIG. 10. Vibrational temperature as a function of argon gas pressure for a 355-nm laser wavelength.

presence of helium gas helps in the cooling and clustering of species, and in turn increases the dominance of C_2 and higher carbon clusters (fullerenes) with increasing helium gas pressures. The presence of argon gas increases the vibrational temperature of the C_2 species. Figure 10 shows the variation of vibrational temperature with argon gas pressures for a 355-nm laser wavelength. However, it can be seen from the figure that the vibrational temperature attains a maximum value at 1 Torr of argon gas, then decreases with a change of pressure on either side. It follows that the higher vibrational temperature at 1-Torr argon gas pressure may lead to the fragmentation and ionization of larger clusters formed in the plasma. The fragmentation and ionization may be attributed to a large number of different processes which include collisional activation, charge exchange, electron collision, multiphoton absorption, etc. Although the exact mechanism of the fragmentation and ionization is not known, one or more of these processes lead to the formation of large number of stable molecular carbon clusters. The increase in the density of molecular carbon clusters, in particular C_2 , results in the formation of a more dense film showing DLC character at 1 Torr of argon gas pressure. Hence it looks from our observation like the vibrational temperature calculated from molecular C_2 emission intensity may be one of the controlling

parameters defining the film characteristics.

IV. CONCLUSIONS

In conclusion, we have characterized the carbon thin films and clusters produced using laser vaporization of graphite in the presence of helium and argon gas. Scanning electron microscopy, transmission electron microscopy, selected area electron diffraction, x-ray diffraction, Raman spectroscopy, and IR, UV-visible spectroscopy were used to characterize the films. Both selected area electron diffraction pattern and x-ray diffraction confirmed the presence of diamond in the carbon film deposited at 1 Torr of argon. The fragmentation and ionization of higher clusters formed in the plasma, leading to an increase in C_2 stable species density, seems to be responsible for the formation of diamondlike carbon.

ACKNOWLEDGMENTS

The work was partially supported by the Council of Scientific and Industrial Research (CSIR) and All Indian Council for Technical Education (AICTE), New Delhi. R.K.D. acknowledges University Grants commission, New Delhi for providing financial assistance.

*Author to whom all correspondence should be addressed.

¹D. B. Chrisey and G. K. Hubler, *Pulse Laser Deposition of Thin Films* (Wiley, New York, 1994).

²R. K. Dwivedi and R. K. Thareja, *Surf. Coat. Technol.* **73**, 170 (1995).

³R. K. Dwivedi and R. K. Thareja, *Phys. Rev. B* **51**, 7160 (1995).

⁴E. Narumi, J. Lee, C. Li, S. Hosokawa, S. Patel, and D. T. Shaw, *Appl. Phys. Lett.* **59**, 3180 (1991).

⁵P. T. Murray and D. T. Peeler, in *Laser Ablation: Mechanisms and Applications-II*, edited by John C. Miller and David B. Geoghegan, AIP Conf. Proc. No. 288 (AIP, New York, 1994), p. 359.

⁶Abhilasha, P. S. R. Prasad, and R. K. Thareja, *Phys. Rev. E* **48**, 2929 (1993).

⁷Abhilasha and R. K. Thareja, *Appl. Phys. B* **60**, 63 (1995).

⁸G. Koren, A. Gupta, R. J. Baseman, M. I. Lutwyche, and R. B. Laibwitz, *Appl. Phys. Lett.* **55**, 2450 (1989).

⁹P. S. R. Prasad, Abhilasha, and R. K. Thareja, *Phys. Status Solidi A* **139**, K1 (1993).

¹⁰H. W. Kroto, J. R. Heath, S. C. O'Brien, R. F. Curl, and R. E. Smalley, *Nature* **318**, 162 (1985).

¹¹W. Kratschmer, L. D. Lamb, K. Fostiropoulos, and D. R. Huffman, *Nature* **347**, 354 (1990).

¹²A. F. Hebard, M. J. Rosseinsky, R. C. Haddon, D. W. Murphy, S. H. Glarum, T. T. M. Palstra, A. P. Ramirez, and A. R. Kortan, *Nature* **350**, 600 (1991).

¹³H. Yonehara and C. Pac, *Appl. Phys. Lett.* **61**, 575 (1992).

¹⁴T. Weiske, J. Hrusak, D. K. Bohme, and H. Schwarz, *Chem. Phys. Lett.* **186**, 459 (1991).

¹⁵D. M. Gruen, S. Liu, A. R. Krauss, and X. Pan, *J. Appl. Phys.* **75**, 1758 (1994).

¹⁶R. K. Thareja and Abhilasha, *J. Chem. Phys.* **100**, 4019 (1994).

¹⁷Abhilasha and R. K. Thareja, *Phys. Lett. A* **184**, 99 (1993).

¹⁸Abhilasha, R. K. Dwivedi, and R. K. Thareja, *J. Appl. Phys.* **75**, 8237 (1994).

¹⁹F. Xiang and R. P. H. Chang, in *Novel Forms of Carbon*, edited by C. L. Reaschler, J. J. Pouch, and D. M. Cox, MRS Symposia Proceedings No. 270 (Materials Research Society, Pittsburgh, 1992), p. 451.

²⁰Y. A. Bukovsky, Ye V. Charyshkin, V. P. Korlenkov, and I. N. Nikolaev, *Spectrochim. Acta* **46A**, 517 (1990).

²¹E. A. Rohlfing, D. M. Cox, and A. Kaldor, *J. Chem. Phys.* **81**, 3322 (1984).

²²A. Trivedi, Ph.D. thesis, Indian Institute of Technology, Kanpur, 1994.

²³H. Ajje, M. M. Alvarez, S. J. Anz, S. D. Beck, F. Diederich, K. Fostiropoulos, D. R. Huffman, W. Kratchmer, Y. Rubin, K. Schriver, D. Sensharma, and R. L. Whetten, *J. Phys. Chem.* **94**, 8630 (1990).

²⁴Q. L. Zhang, S. C. O'Brien, H. R. Heath, Y. Liu, R. F. Curl, H. W. Kroto, and R. E. Smalley, *J. Phys. Chem.* **90**, 525 (1986).

²⁵T. Wakabayashi and T. Achiba, *Chem. Phys. Lett.* **190**, 465 (1992).

²⁶D. S. Knight and W. B. White, *J. Mater. Res.* **4**, 385 (1989).

²⁷D. J. Vitkavage, R. A. Rudder, G. G. Fountain, and R. J. Markunas, *J. Vac. Sci. Technol. A* **6**, 1812 (1988).

²⁸R. J. Nemanich, J. T. Glass, G. Lucovsky, and R. E. Shroder, *J. Vac. Sci. Technol. A* **6**, 1783 (1988).

²⁹F. Tuinstra and J. L. Koenig, *J. Chem. Phys.* **53**, 1126 (1970).

³⁰J. Singh, M. Vellaikal, and J. Narayan, *J. Appl. Phys.* **73**, 4351 (1993).